This document is the accepted manuscript version of the following article:
Sadeghi Marzaleh, A., & Steiger, R. (2021). Experimental investigation of OSB sheathed timber frame shear walls with strong anchorage subjected to cyclic lateral loading. Engineering Structures, 226, 111328 (14 pp.). https://doi.org/10.1016/j.engstruct.2020.111328

This manuscript version is made available under the CC-BY-NC-ND 4.0 license http://creativecommons.org/licenses/by-nc-nd/4.0/

Experimental investigation of OSB sheathed timber frame shear walls with strong anchorage subjected to cyclic lateral loading

Abdollah Sadeghi Marzaleh [a)]*, René Steiger [a)]

[a)] Empa, Swiss Federal Laboratories for Materials Science and Technology, Structural Engineering Research Laboratory, Ueberlandstrasse 129, 8600 Duebendorf, Switzerland

* Corresponding author:

Email: abdollah.sadeghi@piniswiss.com

Tel.: +41 43 343 21 24

Fax.: +41 44 377 62 21

1 Introduction

In Central Europe in many cases, the main lateral force resisting systems in multi-story timber buildings are reinforced concrete (RC) shear walls located around the staircases or elevator shafts. The application of RC shear walls in timber buildings as the lateral force resisting system has several drawbacks. For instance, curing of cast-in-place concrete delays the quick assembly of the timber elements. The constructional tolerance of prefabricated timber elements and cast-in-place concrete is in a different order of magnitude. Moisture of concrete adversely affects the mechanical properties and durability of timber. With the aim of overcoming these drawbacks and also of developing a strong timber only lateral load resisting system, which in particular for regions of low to moderate seismicity is a valuable alternative to RC shear walls, a number of strong sheathed timber frame shear walls (STFSW) located in the perimeter of the multi-story timber buildings running over their full height could be assigned to act as the only lateral force resisting system. For that purpose, the necessary modification of the established configurations of light-frame timber shear walls (LFTSW) was studied by the authors in a research project. The modified timber shear walls were named LFTSWs with strong anchorage by the research team in the first part of the study, where the general behavior of the LFTSWs with strong anchorage under monotonic lateral loading was investigated [1]. The study presented in this paper focuses on the in-plane *cyclic* behavior and seismic performance of the modified timber shear walls, in addition to the further investigation of their in-plane stiffness in the serviceability limit state. Since, compared to conventional light-frame timber shear walls, the modified walls are not light, the more appropriate term "sheathed timber frame shear walls" (STFSW) is used in this paper for the modified LFTSWs.

According to the existing standards ([2], [3]), the seismic response of LFTSWs is experimentally investigated with cyclic racking tests. Regarding the test setup, the boundary conditions should represent the actual stress state of LFTSWs in timber buildings as close as

possible. In the literature, however, the racking tests are commonly performed simply by applying cyclic lateral forces to the top of the walls, which are occasionally preloaded with a constant vertical compressive force. The response of timber shear walls to the in-plane lateral loading has been investigated among others in the studies [4] and [5], in which numerical and analytical models have been developed for different types of timber shear walls and the force-based seismic design of them has been explained. From the research on the effect of vertical force on the shear response of LFTSWs ([6], [7], [8]), it can be concluded that vertical forces significantly improve the shear resistance of LFTSWs only if a rocking mode of failure is governing.

In multi-story buildings, in addition to the vertical force, LFTSWs are likely to simultaneously experience bending moments due to the lateral forces caused by seismic actions and wind. The amount and direction of the bending moment depend on the boundary conditions of the walls. There are a few studies that have taken these conditions into consideration ([9], [10], [11]). Ceccotti et al. [9] investigated the effect of boundary conditions and vertical force by performing a series of experiments on cross-laminated timber (CLT) panels, in which the floor slab was included in the test setup. For an 80% increase in the vertical force, they observed a relatively higher lateral load carrying capacity (~55%) and a rather lower ultimate displacement (~72%). Dujic et al. [12] explained three different patterns of wall behavior, including rocking, rocking-shear, and shear, depending on the boundary conditions of the walls. Partial anchorage of the walls to the foundation was found to be highly influential on the response of the walls. This is not the case in the STFSWs investigated in this research, where rocking is hindered by strong anchorages connecting the edge studs to the foundation by means of multiple steel dowelled connections and slotted-in steel plates. Therefore, in the present study, a more realistic behavior of STFSWs is studied by applying a combination of bending moment and vertical force depending on the story level, in which the wall is located.

To identify the seismic response of STFSWs using quasi-static cyclic lateral forces, the established procedure is to consider a standardized loading protocol, which is representative of the cumulative damage demand. As can be taken from literature, several loading protocols have been developed and implemented in experimental investigations. Some frequently used loading protocols are: SPD [13], CUREE [14], and ISO 21581[3]. Gatto and Uang [15] extensively investigated the behavior of STFSWs under the aforementioned loading protocols and found a significant influence of those on the shear response of timber walls. The number of lateral loading cycles was described as one of the most influential contributing factors in lowering the shear resistance of the timber shear walls. These loading protocols as well as the others reported in literature have been mostly developed for high seismicity regions, where a higher cumulative damage demand is expected. In low-to-moderate seismicity (LMS) regions, such as Central Europe, the above loading protocols represent a level of lateral loading whose demand in shear resistance and ductility of the walls is extremely high and hence, resulting in uneconomical structural designs and retrofit solutions [16]. In an accompanying module of this research [16], a loading protocol was developed especially for regions with low-to-moderate seismicity. In the experimental study presented in this paper, the shear response of STFSWs has been investigated under LMS and ISO loading protocols.

The experimental program in this study provides information about the in-plane cyclic behavior of sheathed timber frame shear walls with strong anchorage subjected to quasi-static monotonic and cyclic lateral forces with various loading protocols. In addition to the lateral loading, the walls were simultaneously loaded with a combination of vertical force and bending moment. Data gathered from the experiments may serve for verifying analytical design approaches and numerical models.

2 Material and method

2.1 Wall specifications

2.1.1 Materials, global geometry, and dimensions

The STFSW, investigated in this study (Fig. 1) was designed force-based according to the Swiss standard SIA 265 [17] and the Eurocode 5 (EN 1995-1-1) [18] design method A. For estimating the seismic action on the STFSW, the equivalent force method was applied and a behavior factor of 2 was taken into account similar to conventional LFTSWs used in Europe. The wall was 2.50 m long and 2.80 m high. The thickness of the STFSWs was chosen as 210 mm, which is approximately 1.5 to 2 times greater than that of typical LFTSWs. Having framing members with a higher cross-sectional area results in a higher in-plane stiffness of the walls. This is compatible with the aim of the study of having a few but stiff STFSWs as the only lateral force resisting system in multi-story timber buildings and allows applying a sufficient amount of thermal insulation between the sheathing panels if needed due to the local climatic conditions prevailing. The framing in the vertical direction consisted of two edge studs, a center stud, and two intermediate studs with cross-sections of 180×180 mm^2, 100×180 mm^2 and 60×180 mm^2, respectively. The top and bottom rails of the framing had a cross-section of 180×180 mm^2. Glued-laminated timber (GLT) of strength class GL24h [19] was used in all framing members. The edge studs were connected to the top and bottom rails from the side of the wall using two long self-tapping screws, which guarantee a stable state of the frame when attaching the sheathing panels to the framing members during production. On both sides of the wall, two OSB/3 sheathing panels ([20], [21]) with a width of 1.25 m, a height of 2.80 m, and a thickness of 15 mm were stapled to the framing members. The geometrical and mechanical properties of the staples were as follows: diameter $d = 1.53$ mm, length of the shanks $l = 55$ mm, and steel grade $f_u \geq 600\,\text{MPa}$. The spacing of the staples was 50 mm except for the intermediate studs

where the spacing was 100 mm. It is worth mentioning that it is commonplace in Switzerland to use staples to connect the sheaths to the frame because of their lower cost and rapid execution, compared to nails. Even though nails could provide a higher shear resistance and a better energy dissipation, the staples are expected to be sufficient for low to moderate seismicity regions.

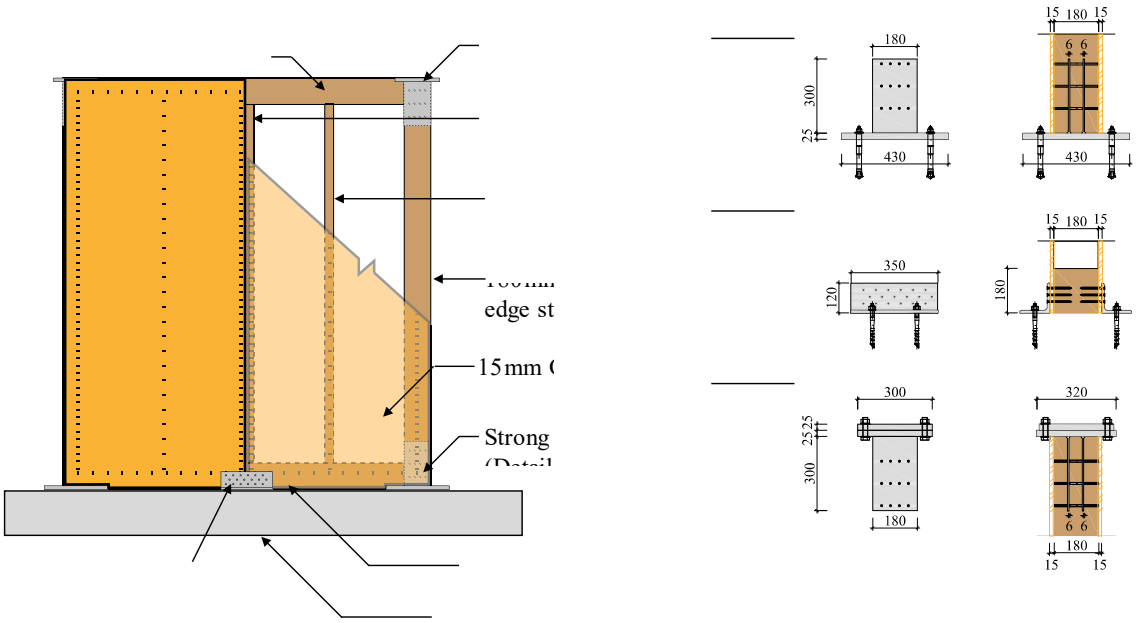

Fig. 1 Configuration of the OSB sheathed timber frame shear walls (STFSW) investigated in the present study.

Strong anchorage was realized with slotted-in steel plate assemblies with two S235 steel plates embedded in the edge studs of the framing (Detail A and C in Fig. 1). Twelve steel dowels were used in these slotted-in connections having a diameter of 8 mm and a tensile strength of $f_u \geq 500\,\text{MPa}$. In addition to the strong anchorages, a shear connector (Detail B in Fig. 1) was installed at the mid-length of the wall on both sides. The shear connectors contributed in transferring the shear forces to the foundation. M16 undercut anchors and M16 capsule adhesive anchors were used to anchor the slotted-in steel plate and shear connectors, respectively, to the reinforced concrete foundation. The executed slotted-in connection and shear connector can be seen in Fig. 2.

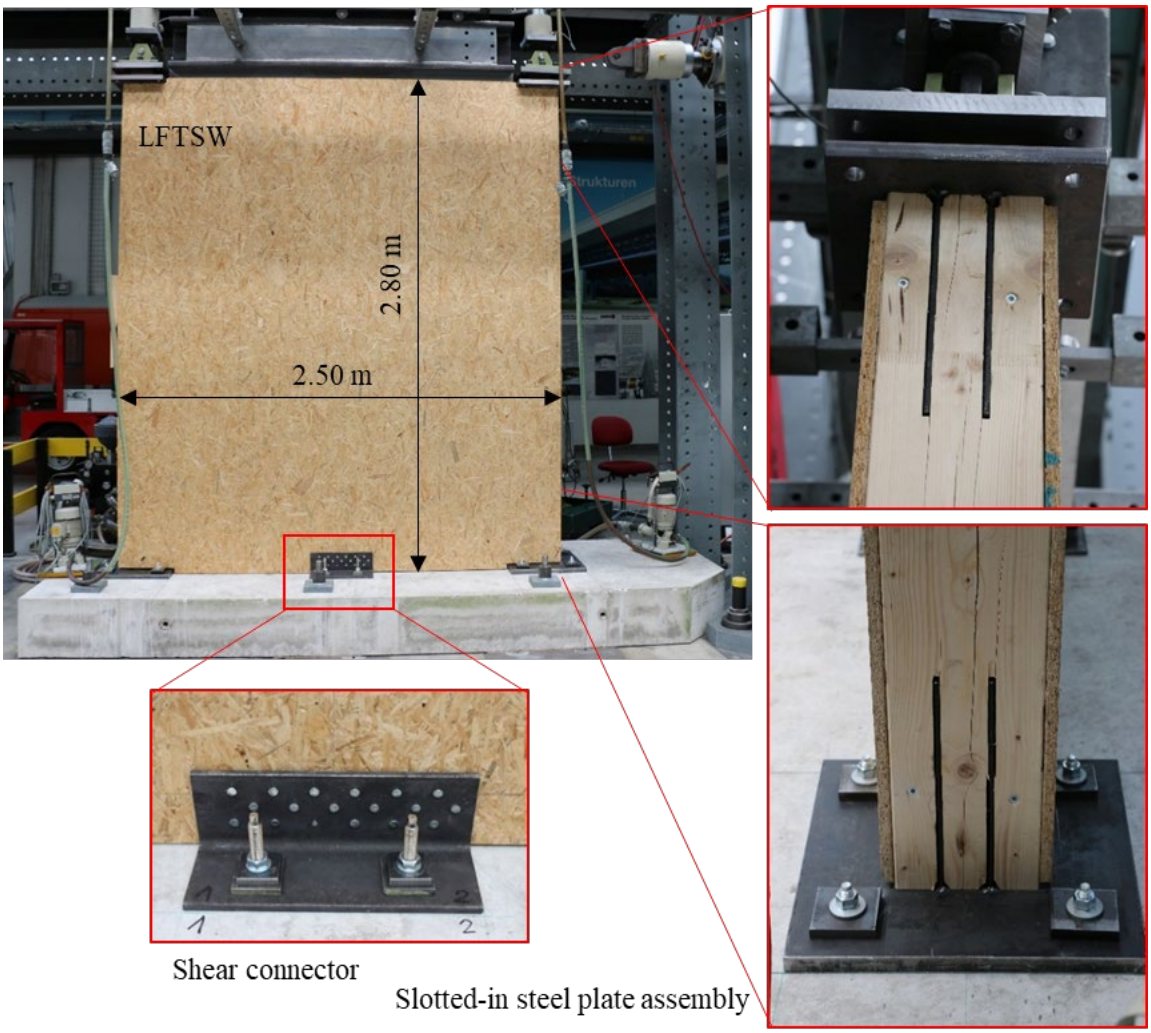

Fig. 2 Sheathed timber frame shear wall (STFSW), L-shape shear connector, and slotted-in steel plate assemblies were used for anchoring the STFSW to the foundation.

2.1.2 Constructional detailing

Despite having identical global geometry, the STFSWs had an important difference in constructional detailing at their corners, where the OSB panels met the slotted-in steel plates in the anchorages. In the tests under high vertical force (cf. Table 1), a gap was designed at the mentioned location to avoid contact of OSB panels and steel plates. The rest of the specimens were produced lacking the gap between the OSB panels and the steel plates. Fig. 3 shows the gap in the specimen HV-WOB as opposed to the specimen LV-WOB, in which there was no gap.

Having a gap between sheathing panels and adjacent wall elements, was also taken into consideration by Varoglu et al. [22] in their experiments aiming at not restraining the rotation

of sheathing panels. Leaving a gap is recommended by APA [23] in order to prevent premature buckling of the OSB panels that could happen due to compressive stresses in the OSB panels. When there is no gap between the elements in a STFSW, compressive stresses can be generated in the panels even due to changes in moisture content of the panels during erection if not adequately acclimatized. If there would be no gap, the OSB panels, when subjected to lateral loading, may come into contact with the steel plates. This constrains the rotation of the OSB panels and leads to a contribution to in-plane stiffness of the specimen difficult to quantify and, at high levels of acting forces, may cause local buckling of the OSB panels. Leaving a gap is, however, a procedure not systematically applied in practice.

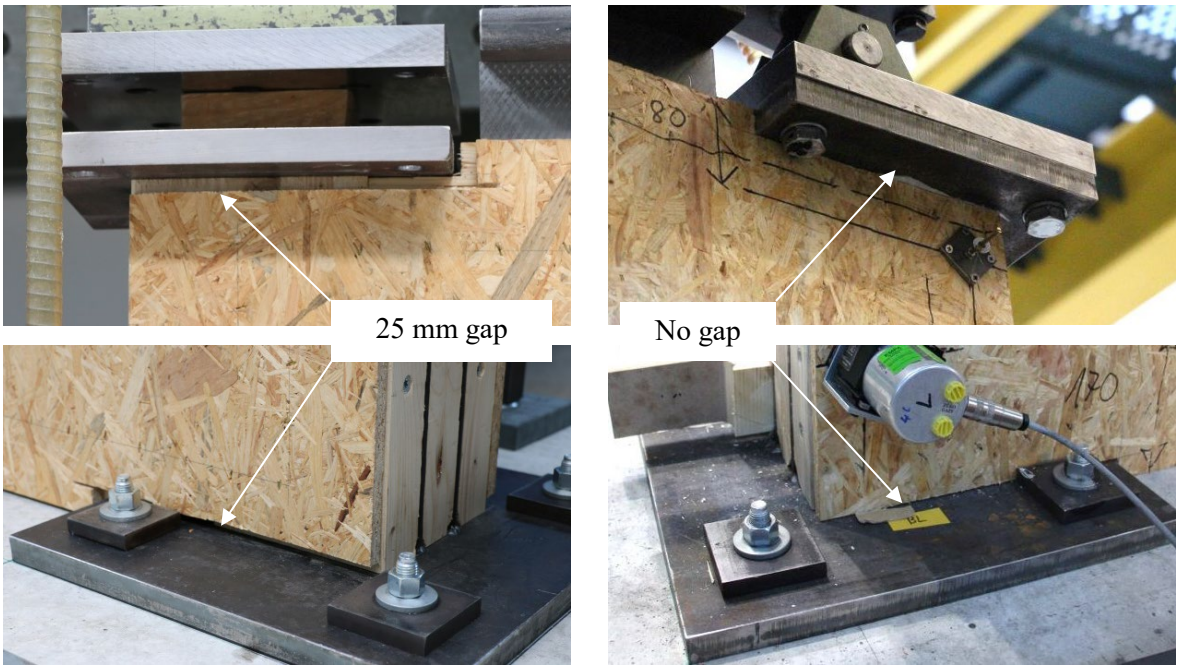

Fig. 3 Difference in constructional detailing of sheathing panels leaving a gap between the sheathing panel and the steel anchorage plate: (a) a large gap in test specimen HV-WOB and (b) a small gap in test specimen LV-WOB.

2.2 Loading

The seismic response of STFSWs was investigated in a series of experiments (Table 1). Fig. 4 illustrates the reference four-story building considered for estimating the forces on the STFSWs to be applied in the test series. The focus of the test program was on studying the influence of

154 the following parameters: (i) level of vertical force (L: low or H: high), (ii) bending moment
155 (W: with or WO: without), and (iii) lateral loading protocol (ISO or LMS). These parameters
156 are addressed in this section in more detail.

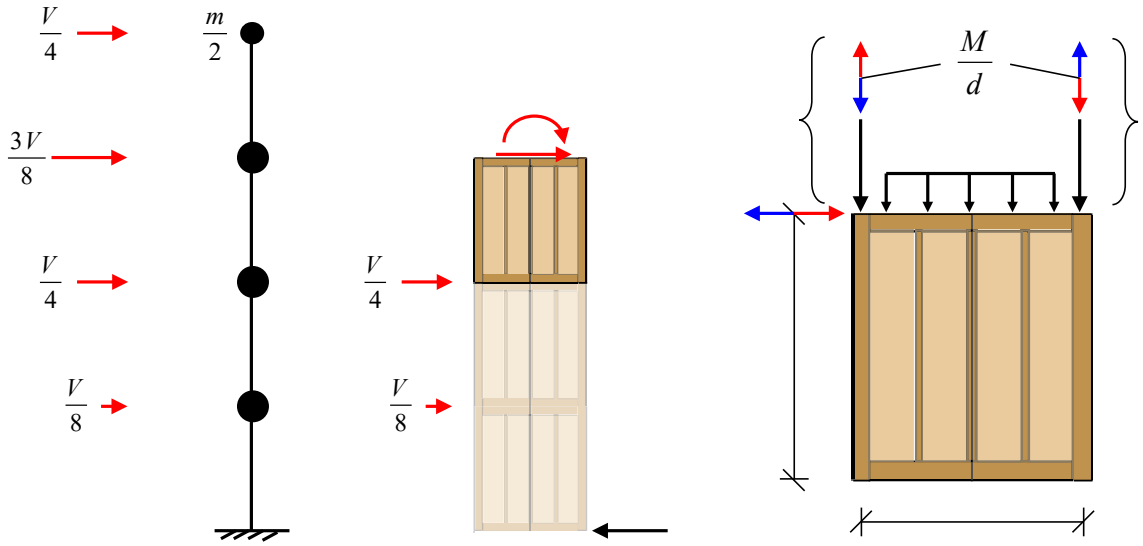

157 Fig. 4 The reference four-story building with a simple triangular distribution of the base shear in elevation and the
158 corresponding forces acting on the STFSW located in the 2nd floor.

159

160 Table 1: Test plan under various actions: distributed vertical force (N), initial concentrated vertical force at the
161 edge studs (F_v), lateral force (P), and bending moment (M) (as depicted in Fig. 4).

Test	**Vertical forces**		**Bending moment-shear force ratio**	**Lateral loading protocol**
	N (kN)	F_v (kN)	$\frac{M}{P}$	P
LV-WOB	60[1)]	15	0	Monotonic, ISO 21581 [3]
HV-WOB		123	0	Monotonic, ISO 21581 [3]
HV-WOB-ISO		123	0	Cyclic, ISO 21581 [3]
LV-WB		15	$0.4h$ [2)]	Monotonic, ISO 21581 [3]
LV-WB-ISO		15	$0.4h$	Cyclic, ISO 21581 [3]
LV-WB-LMS		15	$0.4h$	Cyclic, Mergos and Beyer [16]

162 [1)] This value includes the dead load of the force transfer beams in the test setup shown in Fig. 6.

163 [2)] h = Story height

164

2.2.1 Vertical force

In order to investigate the effect of vertical force on the shear response of STFSWs, two load levels were applied to the walls. The two load levels, labelled "low" and "high", were estimated assuming the wall being respectively in the 2nd floor and the ground floor of a typical 4-story timber building in Switzerland. These buildings in most cases are realized with timber concrete composite (TCC) slabs with spans between 4 m (residential building) and 8 m (office building) settled on sheathed timber frame walls. The reader is referred to Steiger et al. [24] for more information about the constructional details and loading in this type of buildings.

In the investigated type of multi-story timber buildings, floor slabs are connected to timber shear walls in a way that the vertical load of the slabs is transferred to the walls via top rails. The STFSWs of different stories are connected to each other at the location of the edge studs by means of the previously explained embedded steel plates. Therefore, it can be assumed that the vertical forces of the upper stories are transferred to the edge studs of the STFSWs in the considered floor. As a result, two separate parts of vertical loading were considered in the experiments being: 1) a distributed force on the top rail (**Error! Bookmark not defined.** N) accounting for the vertical load of the story located right on top of the wall and 2) two concentrated vertical forces acting on the edge studs representing the vertical forces of the rest of stories located above the investigated floor.

2.2.2 Bending moment

In addition to the vertical force, the shear walls in multi-story buildings experience a bending moment due to the lateral forces on upper stories. To have a better representation of the seismic actions on STFSWs, the resultant bending moment was considered in the experimental study. For simplicity, the lateral loading pattern was calculated by distributing the base shear force along the elevation of the typical 4-story building, assuming equal lumped masses in all story levels except for the roof level, where in the type of buildings studied usually an attic story is

located and hence, simply half of the mass of the other stories was assigned (see Fig. 4). Based on the considered horizontal loading pattern, the ratio between the bending moment on top of the wall and the shear force was estimated as 40% of the wall height (equivalent to a shear span to wall height ratio of 1.4). The corresponding bending moment was applied to the wall specimens using the vertical servo-hydraulic actuators in form of a pair of coupled forces acting in opposite directions. Therefore, the total force in the vertical actuators, including the concentrated vertical forces amounted to:

$$F_1 = -F_v - 0.4P\frac{h}{d} \quad \text{and} \quad F_2 = -F_v + 0.4P\frac{h}{d}$$

with F_v={15;123}.

where P stands for the applied lateral force, h for the story height, and d for the distance between the vertical servo-hydraulic actuators. In the above formulas, the compressive force in the actuators was taken as negative.

In the tests under high vertical force (HV), more than 75% of the capacity of the vertical servo-hydraulic actuators was used for applying the vertical forces. Therefore, the bending moment was only applied in tests under low vertical force (see Table 1).

2.2.3 Loading protocol

The existing loading protocols, such as the sequential phased displacement (SPD) protocol [13], the CUREE protocol [14], and the ISO 21581 protocol [3], are based on recordings gathered in regions with high seismicity. Since, the load-carrying and deformation capacity of timber shear walls depend on the imposed demand, as highlighted by Krawinkler et al. [14] and Gatto and Uang [15] among others, implementing these loading protocols may underestimate the capacity of timber frame shear walls designed for applications in low to moderate seismic regions.

In the study presented in this paper, STFSW specimens were subjected to the ISO 21581 protocol as well as the loading protocol for regions in Central Europe with low-to-moderate seismicity (LMS), developed by Mergos and Beyer [16], in order to assess the influence of the loading protocols on the seismic behavior of the STFSWs. Since theses protocols are defined based on the ultimate displacement capacity of the walls, before executing the cyclic tests, prerequisite monotonic tests were performed on the walls based on the ISO 21581 monotonic loading protocol [1].

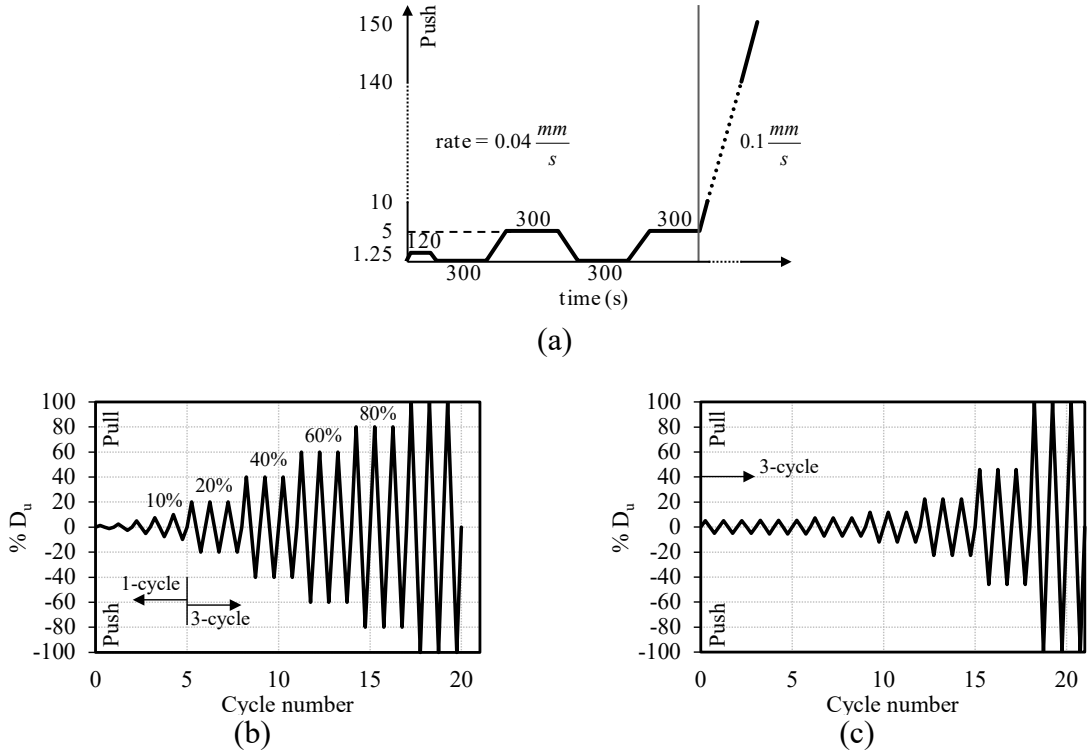

Fig. 5: Loading protocols applied in the experiments: (a) monotonic ISO 21581 [3], (b) cyclic ISO 21581, and (c) cyclic low-to-moderate seismicity (LMS) [16] (D_u is the ultimate displacement obtained in the monotonic tests [1]).

Fig. 5 illustrates the loading protocols used in the experimental program consisting of (i) the monotonic ISO 21581 loading protocol (Fig. 5(a)), (ii) the cyclic ISO 21581 protocol (Fig. 5(b)) and (iii) the loading protocol for cyclic low-to-moderate seismicity (LMS) [16] (Fig. 5(c)). In the ISO 21581 loading protocol, the amplitude of the phases increases stepwise. In the newly developed LMS loading protocol, however, the amplitudes follow an exponential function

228 resulting in low amplitude initial cycles and high amplitude final cycles. Comparing the
229 ISO 21581 and LMS loading protocols for a nearly equal number of cycles (20 for ISO 21581
230 and 21 for LMS), the total displacement demand is relatively lower by the LMS protocol than
231 the ISO 21581 protocol. Therefore, compared to tests under the ISO 21581 protocol, less
232 damage is expected to occur in tests under the LMS protocol.

233

234 3 Test setup

235 The main components of the test setup are shown in Fig. 6. Deviating from usual setups applied
236 for such tests and in order to get a test situation as close to practice as possible, the wall
237 specimens were not anchored to a steel beam but rather to a reinforced concrete slab which was
238 connected to the strong floor of the laboratory with prestressed bolts. The STFSW specimens
239 were anchored to the concrete foundation on both edges through the embedded slotted-in steel
240 plate assemblies shown in Fig. 2. The shear connectors were put in place, nailed to the wall,
241 and connected to the foundation using bolts.

242 A reaction frame was assembled on the strong floor providing the support for the hydraulic
243 cylinders. Two different types of hydraulic cylinders were used in the experiments namely usual
244 hydraulic jacks and servo-hydraulic actuators, hereinafter referred to as actuators. The hydraulic
245 jacks (shown in green in Fig. 6) applied the distributed vertical force (N) to the test specimens,
246 whereas the adjacent actuators applied the concentrated vertical loads (F_v) in combination with
247 the coupled forces of the bending moment (F_1 and F_2). The transfer of the distributed vertical
248 force was realized with a concrete beam supported vertically by three steel rollers on top of a
249 steel beam. The steel beam was bolted to a stiff steel plate, which was rigidly connected to the
250 top rail of the walls using 120 self-tapping screws with a diameter of 10 mm and a length of
251 180 mm. Therefore, no slip was to be expected in the connection between the steel beam and

the wall specimens. The steel rollers allowed for a free horizontal movement under lateral force without transferring any horizontal forces to the vertical hydraulic cylinders. Out-of-plane displacement of the steel beam was prevented by means of a system of lateral supports. The horizontal cyclic force (P) was applied to the wall using the horizontal actuator, which was connected to the steel beam on the one side and to the rigid steel reaction frame on the other side. The two vertical actuators were mounted with a hinge to the slotted-in steel plate connections embedded in the edge studs of the walls. The three servo-hydraulic actuators were operated by means of a Digital 3-Channel Control System PCS 8000. The components of the test setup, especially those located on top of the wall for introducing the loads and stabilizing the specimen, are explained in more detail in Sadeghi Marzaleh et al. [1].

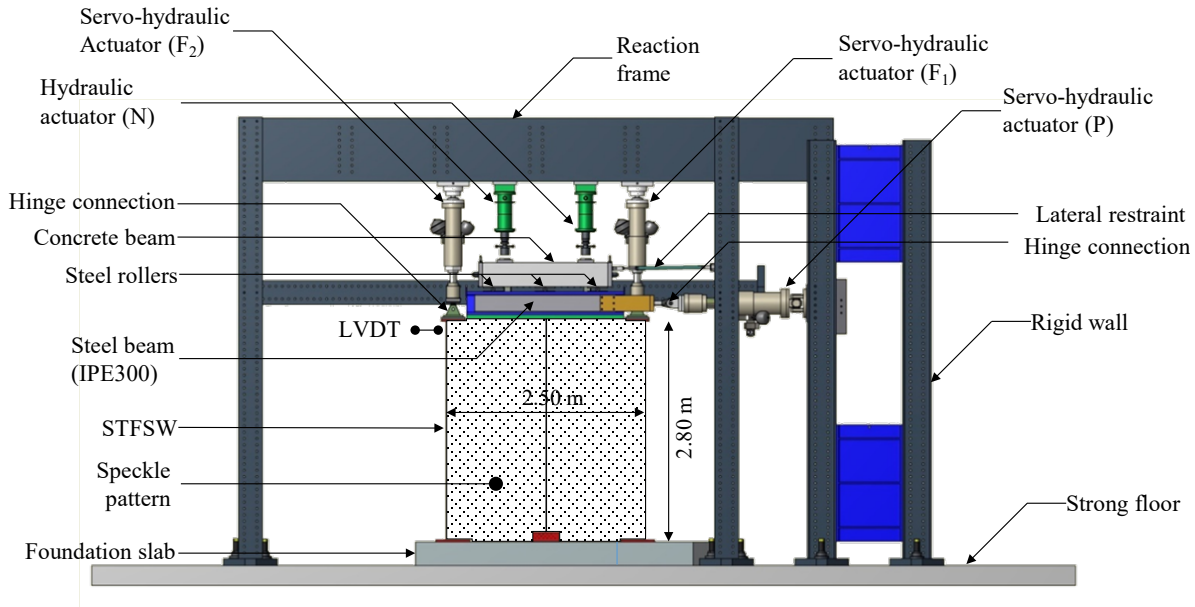

Fig. 6 Test setup with emphasis on the force introduction system using hydraulic jacks (inner pair, green) for applying the distributed vertical force (N) and servo-hydraulic actuators (outer pair, linen) for applying the concentrated vertical forces and bending moment (F_1 and F_2) as well as the shear force (P).

3.1 Measurements

The elongation and shortening of each panel is representative of the amount of tensile and compressive stresses being transferred through the panel to the foundation. To measure these parameters, two string potentiometers were installed diagonally on each OSB panel on one side

of the wall. To assess the full stress distribution in the OSB panels, a 3D digital image correlation (DIC) system was used on the opposite side of the wall, with which the full-field displacement of the panels was measured. The applied 3D DIC system was a commercial GOM system composed of two 4 MP stereo cameras with a focal length of 20 mm which were placed horizontally at a distance of 1.34 m from one another in a plane parallel to that of the wall specimen. The distance of the cameras to the specimen was equal to 4.48 m to cover the entire surface of the wall. A speckle pattern was painted on one side of the wall for the optical measurement (see Fig. 6). The displacement of the framing members is different from that of the sheathing panels. To measure the framing displacement, several timber plates were screwed to the edge studs on each side of the wall. These timber plates were also painted with a speckle pattern, so that their displacement could be measured with the 3D DIC system. The number of timber plates attached to the framing was increased in some of the experiments in order to have more measurement points on the framing and hence, to get a better resolution of the displacement measurements of the framing.

In addition to the strain measurement mentioned above, the horizontal deformation of the wall was measured with a displacement transducer located at the top corner of the walls on the side opposite to the horizontal actuator. The force and displacement of the actuators were also measured continuously during the experiments.

3.2 Test procedure

In the first stage, the distributed vertical force was applied to the walls by increasing the oil pressure in the cylinders. Then, the concentrated vertical forces F_1 and F_2, only due to the vertical load, were applied to the wall acting on the edge studs. No bending moment was applied to the wall until this stage. Subsequently, the horizontal loading (P) was initiated according to the loading protocol under investigation and continued until failure. The concentrated vertical

293 forces (F_1 and F_2) were updated simultaneously as a function of the horizontal force in order to
294 apply the bending moment. Even though in the standard ISO 21581 [3] the failure of a shear
295 wall specimen is defined as 20% degradation in the shear resistance, the tests were continued
296 to higher values of degradation in order to observe the behavior of the wall specimens in the
297 post-peak range. It was only in the first test, HV-WOB, that the test was stopped earlier (at 15%
298 degradation) because the maximum stroke of the horizontal actuator had been reached.

299 4 Results and discussion

300 4.1 In-plane behavior, damages and failure modes

301 To explain the response of the STFSWs under cyclic horizontal loading, it is worthwhile to first
302 analyze their response under monotonic loading. Thus, in this section, the monotonic response
303 of the walls is explained in detail. The differences regarding the cyclic response will be
304 highlighted successively.

305 4.1.1 Monotonic tests

306 Fig. 7 illustrates the general in-plane behavior of the walls under monotonic horizontal loading.
307 To better explain the behavior of the wall under monotonic loading, four states are highlighted
308 in the diagram and their corresponding total in-plane displacements are illustrated. The
309 horizontal force and displacement reported here are those, measured respectively by the load-
310 cell of the horizontal actuator and the LVDT depicted in Fig. 6. The reported total in-plane
311 displacements are based on the results of the 3D DIC measurement of the sheathing panels and
312 the framing members.

313 In the first phase of the experiment after applying the distributed and concentrated vertical
314 forces, no damage was visible in any of the specimens during the experiments. Subsequently,

315 the horizontal displacement was applied to the steel beam that was directly transferred to the
316 top rail, pushing one of the edge studs and pulling the other one in the lateral direction. In fact,
317 due to the applied horizontal displacement, the framing members being connected to each other
318 were pushed through the sheathing panels, where the resistance to the relative displacement
319 was provided by the staples. In the early phase of monotonic horizontal loading, because of the
320 strong anchorage to the foundation, the edge studs deform in a cantilever way. Both OSB
321 sheathing panels rotated around the shear connector located in the middle of the wall (blue zone
322 in Fig. 7b). The observed nonlinear force-displacement behavior indicated that the staples
323 located far from the rotational center were subjected to plastic deformations to some extent even
324 in the serviceability limit state (i.e. for top wall horizontal displacements of up to 1/500 of the
325 story height).

326 As shown in Fig. 7c, when increasing the applied horizontal displacement to the top rail, an
327 increase was observed in the rotation of the sheathing panels. As a result, the relative
328 displacement of framing and sheathing panels increased. This gave rise to the number of staples
329 experiencing plastic deformations; therefore, a nonlinear behavior was observed in the global
330 force-displacement behavior, in which the increase rate of the shear resistance decreased. At
331 the corners of the OSB sheathing, depending on the constructional detailing and the size of the
332 gap between the sheathing panels and the steel plates (explained in section 2.1.2), the sheathing
333 panels came into contact with the steel plates that later resulted in crushing of the sheathing
334 panels. The corresponding drop in the force-displacement curve is visible in Fig. 7a. At the
335 location of the shear connector, the embedment of nails in the sheathing panels was more
336 significant in the left panel. This can be observed clearly in Fig. 7c, where the center of rotation
337 of the left panel moved away from the movement constraint of the shear connector.

338 The higher the horizontal displacement applied to the wall, the more staples experienced plastic
339 deformations and the higher the plastic strain in the staples far from the center of rotation until

the peak horizontal force, i.e. the maximum shear resistance, of the walls was reached. It can be seen in Fig. 7d that at this point, the center of rotation of the right panel was still close to the shear connector expressing that the local buckling/crushing of the right OSB panel was yet to happen.

By increasing the applied displacement in the post-peak region, a gradual decrease was observed in the shear resistance of the walls due to the redundancy of the system having numerous staples. When the sheathing panels located close to the shear connector failed due to buckling and crushing, a drop was observed in the force-displacement diagram highlighted in Fig. 7e. It led to a change in the rotational center of the right OSB and moved it away from the shear connector. Even after local buckling of the panel, the decrease in shear resistance of the wall was fairly gradual and no abrupt failure was observed.

After applying the horizontal loading, the walls were moved back to the original position (i.e. zero horizontal displacement) with the horizontal actuator under displacement controlled loading. The STFSWs could resist the distributed and concentrated vertical forces still at this stage and during the whole test program. The reader is referred to [1] for a detailed description of the failure modes.

356

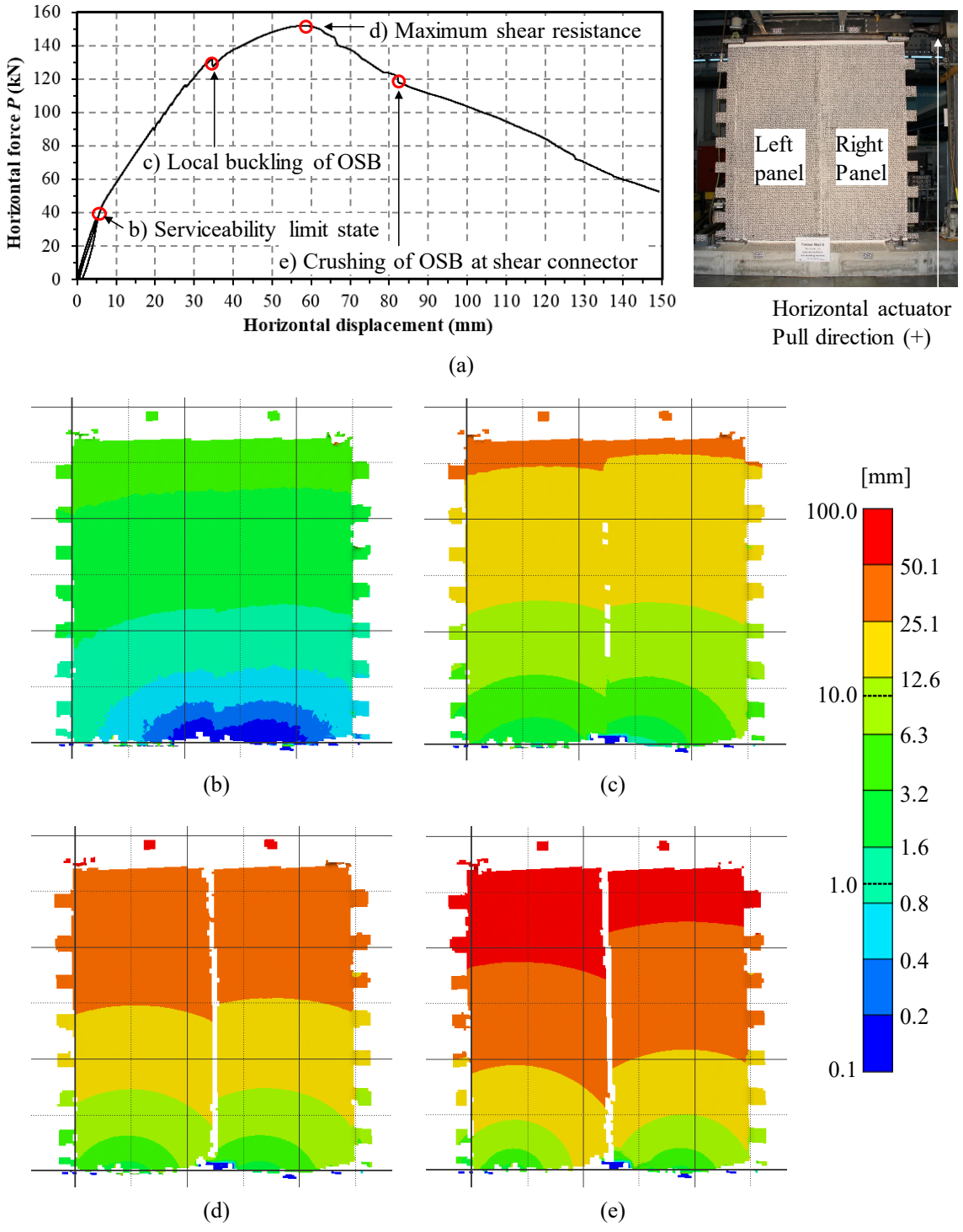

357

358 Fig. 7 (a) In-plane horizontal force-displacement curve of the STFSWs under monotonic loading. The total in-
359 plane displacements of the sheathing panels and the framing are shown in four different states (b-e) marked with
360 red circles in the force-displacement diagram.

361

4.1.2 Cyclic behavior

As shown in Fig. 8, the overall behavior and damages of the STFSWs when subjected to cyclic horizontal loading were similar to those observed in the monotonic tests. The initial nonlinear response of the walls was followed by local crushing of the sheathing panels in both bottom corners, accompanied by a small drop in the horizontal force-displacement diagram. Subsequently, at the location of the shear connector, embedding of the nails in the sheathing panels developed, which resulted in the movement of the center of rotation of the panels away from the shear connector. By increasing the applied horizontal displacement, the walls reached their maximum shear resistance where numerous staples experienced plastic deformations and consequently softening. Afterwards, as opposed to the monotonic tests, no local buckling of the OSB panels was observed in the region close to the shear connector; the observed drop in the force-displacement curve was a result of the buckling/crushing of the OSB panels at their top corners due to getting into contact with the slotted-in steel plates. In the final stage, the majority of staples connecting the panels to the mid-stud were pulled out accompanied by a very low shear strength of the STFSW. The final state of the STFSWs after removing the horizontal and vertical forces as well as corresponding damages are shown in Fig. 9. For a comparison of the damages experienced in the monotonic tests, the reader is referred to [1].

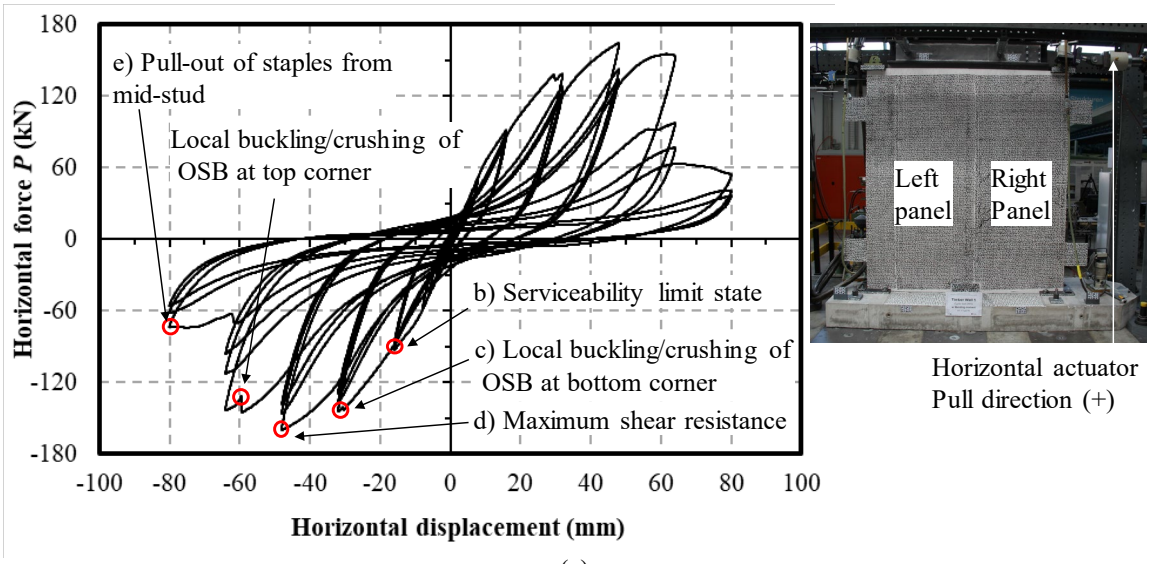

(a)

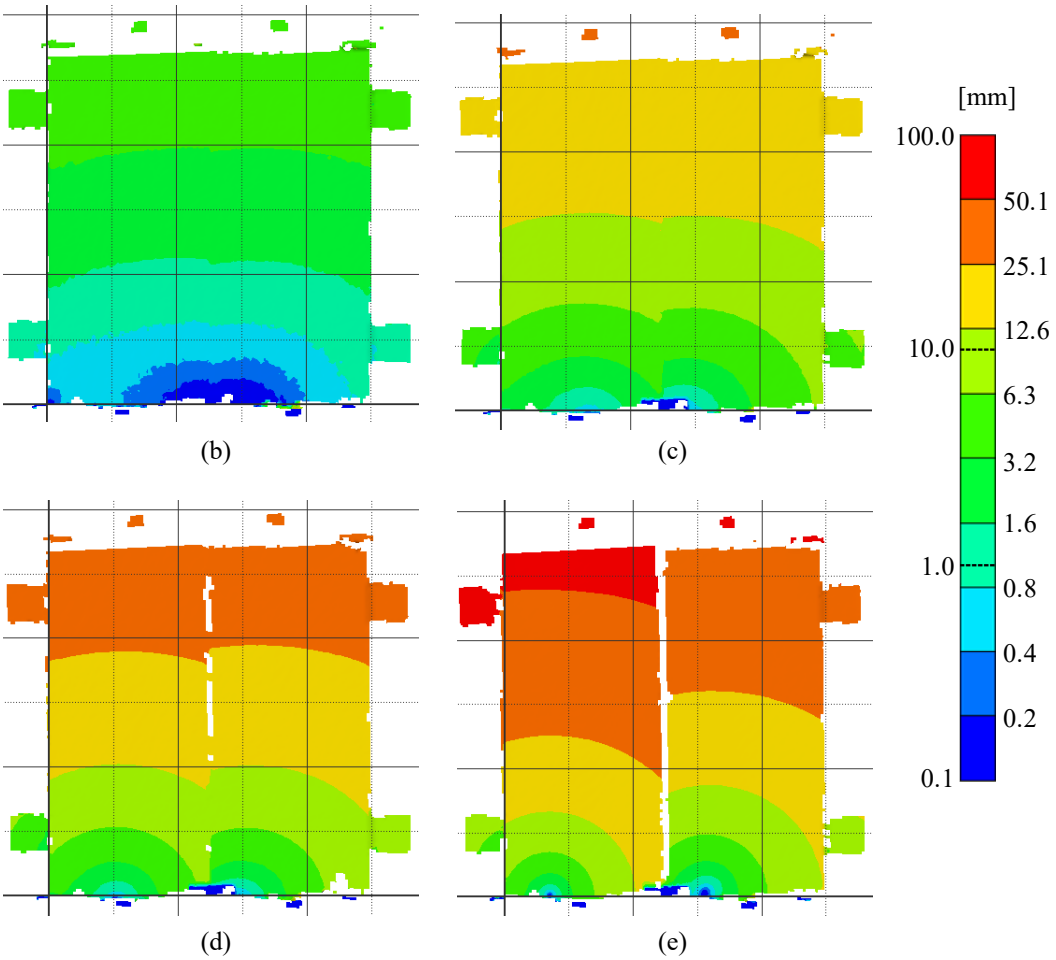

(b) (c)

(d) (e)

379

380 Fig. 8 (a) In-plane horizontal force-displacement curve of the STFSWs subjected to cyclic loading. The total in-
381 plane displacements of the sheathing panels and the framing are shown in four different states (b-e) marked with
382 red circles in the force-displacement diagram.

383

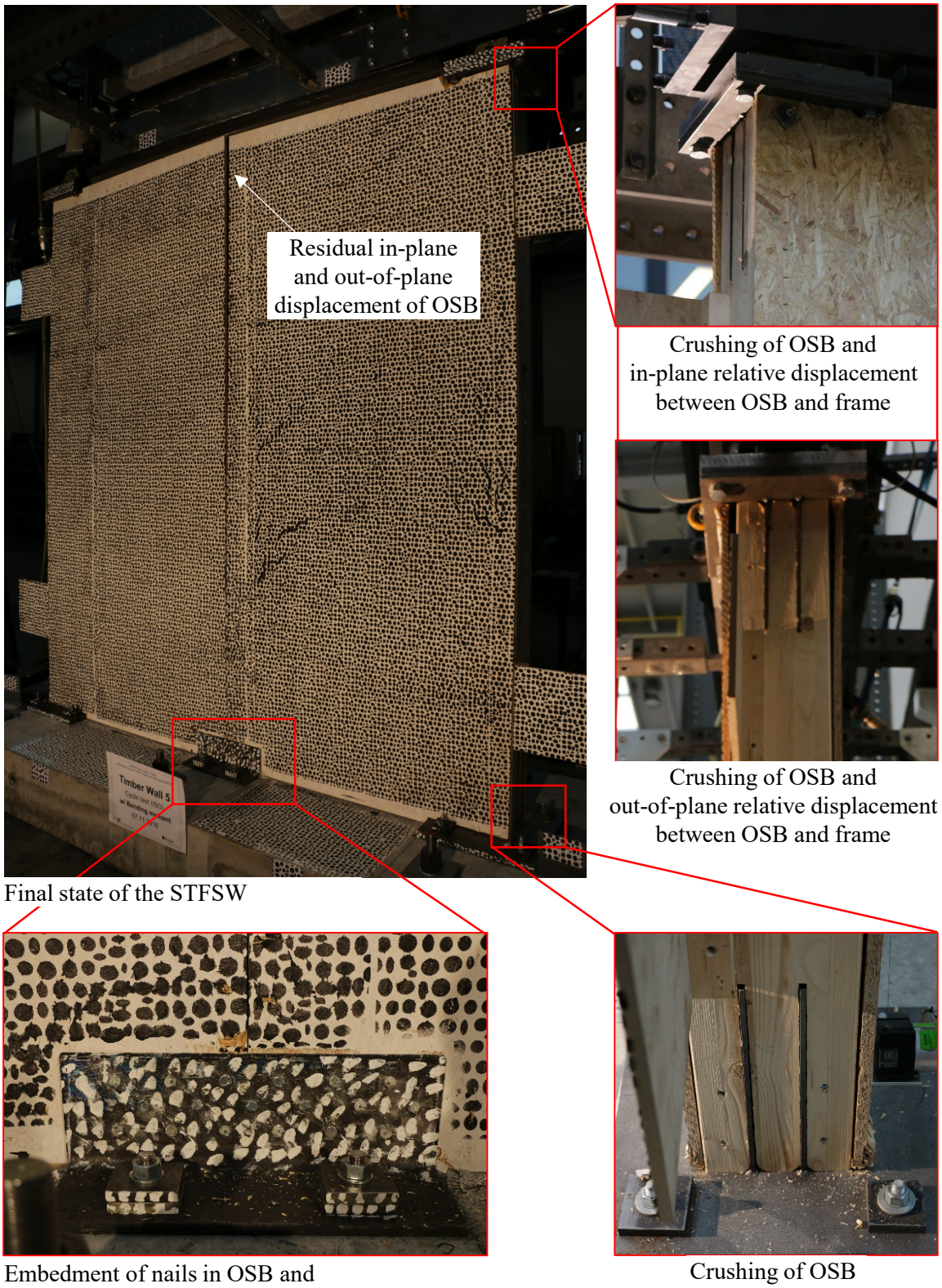

384

385 Fig. 9 Damages in the STFSWs subjected to cyclic loading after the experiment.

386

387 The major difference between the response of the STFSWs under monotonic loading and cyclic
388 loading was identified in the post-peak region, where the failure occurred at a significantly
389 lower displacement under cyclic loading. This finding agrees with the results of the monotonic
390 and cyclic tests performed on LFTSWs with various sheathings by Dolan and Toothman [25].
391 For the case of OSB sheathings, the authors stated that the walls did not perform as well as
392 under monotonic loading when subjected to cyclic loading. They reported an 18% decrease in
393 the ultimate displacement measured in the cyclic tests compared with the monotonic ones.

394 In the present study, the gradual post-peak behavior under monotonic loading was changed to
395 a significant drop in the shear resistance of the walls by repeating the first cycle in the post-
396 peak region. This can be explained better by observing the out-of-plane deformations of the
397 sheathing panels, especially in the cycle where the maximum drop in the shear resistance
398 occurred. Fig. 10 shows the development of the out-of-plane deformations of the wall in the
399 first post-peak cycle. As can be seen in the figure, before this cycle, only a very limited and
400 local out-of-plane displacement had occurred. Increasing the applied horizontal displacement
401 in a cyclic way, due to the pulling-out of the staples, the out-of-plane displacements
402 significantly increased. Since the contribution of the pulled-out staples in the shear resistance
403 of the wall was negligible, the shear resistance of the wall dropped significantly in the second
404 and third cycle.

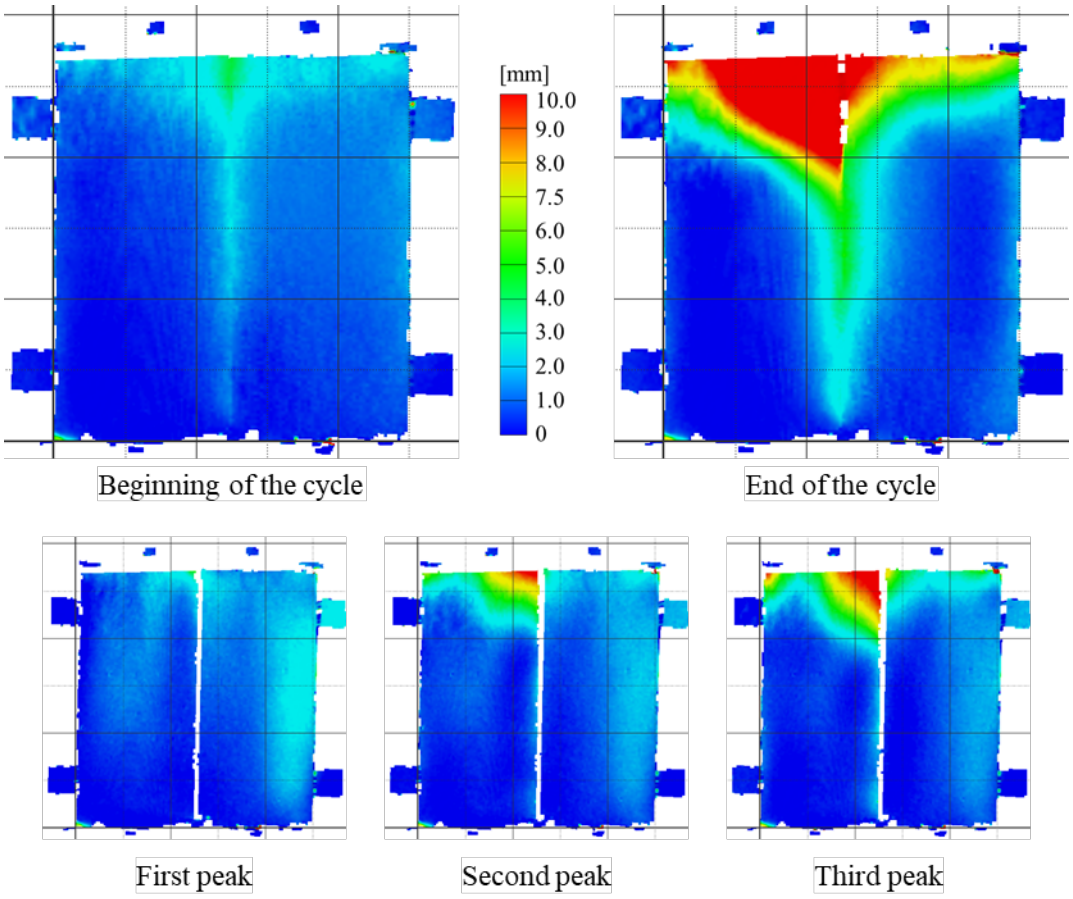

405

406 Fig. 10 Out-of-plane displacement development in the cycle with a significant drop in shear strength (peak values
407 correspond to the pull direction).

408 ## 4.2 Shear stiffness, shear strength, ultimate displacement and viscous damping

409 The hysteresis curves of the cyclic horizontal force-displacement response of all tests are shown
410 in Fig. 11. For comparison purposes, the response of the walls under monotonic loading was
411 included symmetrically in the diagram in the pull and push directions.

412 As shown in Fig. 11, the initial tangent stiffness of the walls under cyclic loading was basically
413 equal to that under monotonic loading. Nevertheless, after several cycles the cyclic behavior
414 was stiffer than the monotonic one. It was followed by a higher shear strength in all the cyclic
415 tests. The cyclic behavior of the walls was also characterized by an evident pinching behavior
416 accompanied by a strength degradation what is to be expected for stapled sheathing to framing
417 connections.

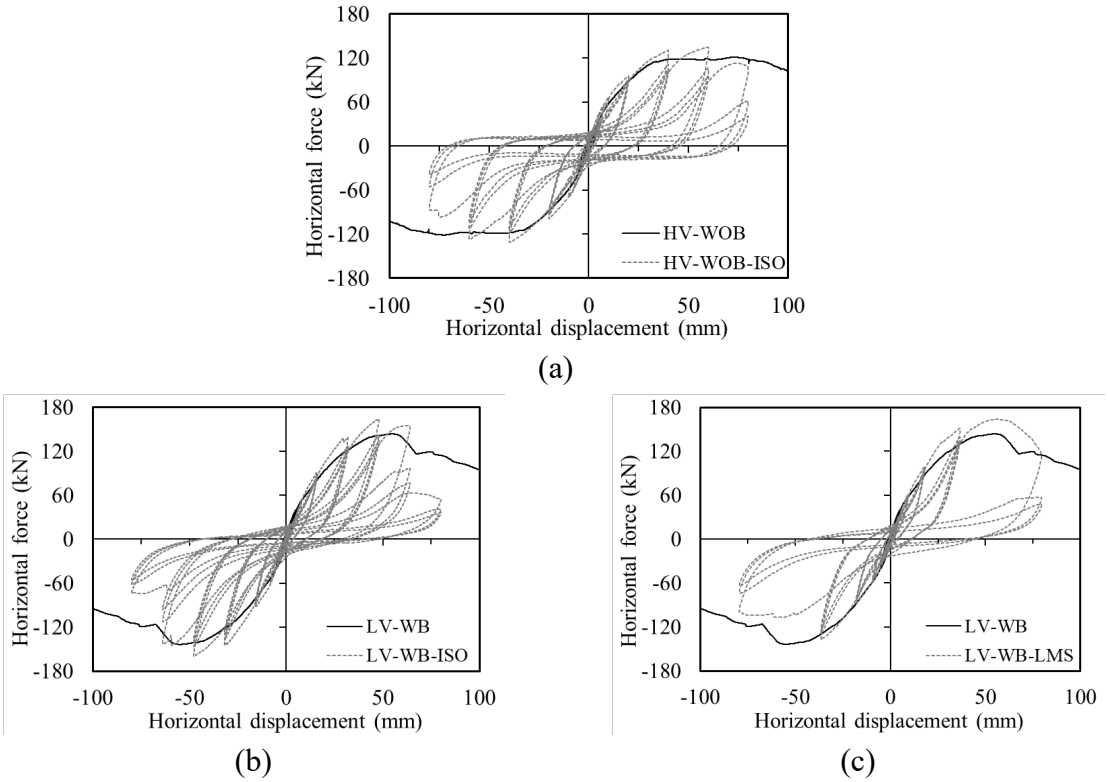

Fig. 11: Hysteretic behavior of STFSWs subjected to (a) high vertical force and ISO 21581 loading protocol (b) low vertical force and ISO 21581 loading protocol, and (c) low vertical force and low-to-moderate seismicity (LMS) loading protocol compared with their behavior when subjected to monotonic loading [1].

Fig. 12 compares the backbone horizontal force-displacement curves derived from the cyclic tests, which were created according to ASTM E2126 [2], with the horizontal force-displacement behavior of the walls under monotonic loading [1]. For the backbone curves, the envelope of the primary cycle of the cyclic tests was considered. A quantitative comparison can be found in Table 2 and is explained in the following.

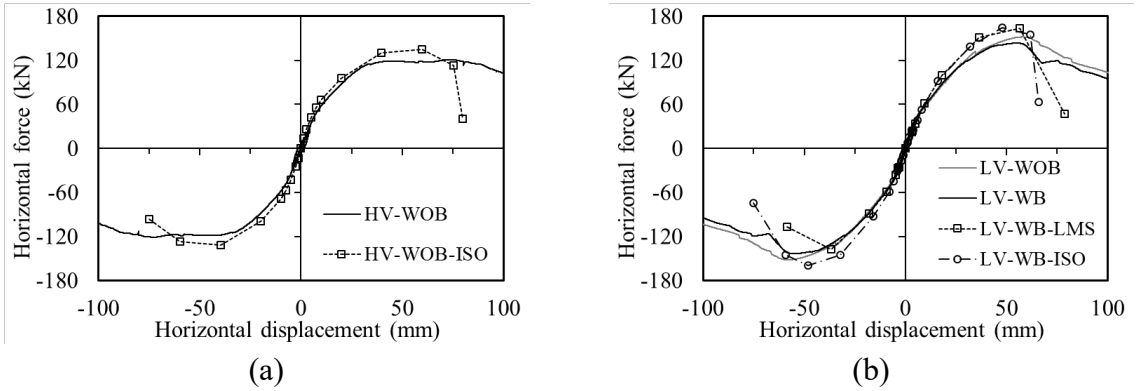

Fig. 12: Backbone envelope curves derived from the cyclic tests in comparison with the force-displacement curves from monotonic tests under (a) high vertical force and (b) low vertical force [1].

Table 2: Secant stiffness ($K_{\mathrm{sec},0-0.4F_{\max}}$), shear strength ($P_{\max}$), displacement capacity (D_u), ductility ratio (μ), and viscous damping (ν_{eq}) of the tested STFSWs estimated according to ASTM E2126 [2].

Test	$K_{\mathrm{sec},0-0.4F_{\max}}$ (kN/mm)		$P_{\max}$ (kN)		D_u (mm)		μ (-)		ν_{eq} (-)
	Push	Pull	Push	Pull	Push	Pull	Push	Pull	
HV-WOB	6.7	-	121	-	99.0	-	6.0	-	-
HV-WOB-ISO	7.9	7.6	131	135	70.9	75.6	4.8	4.8	0.13
LV-WOB	5.9	-	152	-	81.6	-	3.6	-	-
LV-WB	6.7	-	144	-	78.1	-	4.2	-	-
LV-WB-ISO	7.1	6.2	160	165	63.2	62.8	3.2	2.7	0.10
LV-WB-LMS	6.5	6.4	138	164	56.1	62.7	3.1	2.8	0.10

Shear stiffness and strength

The shear stiffness of the STFSWs was estimated according to the procedure specified in ASTM E2126 [2], in which the secant stiffness is calculated between the two horizontal force levels of zero and 40% of the ultimate shear strength.

As can be seen from the values listed in Table 2, the secant stiffness was higher in the cyclic tests than in the monotonic ones (about 18% for the test under high vertical force and 6% for the test under low vertical force conducted with the ISO 21581 loading protocol), except for the test performed with the LMS horizontal loading protocol, in which the secant stiffness was marginally lower (-3%). The ultimate shear strength was always higher (11-15%) in the cyclic tests than in the monotonic ones. This observation is against the widely accepted premise that the monotonic load-displacement curve contains the hysteresis for the timber shear walls ([22]). In the nonlinear analysis of sheathed timber shear walls, it is common to consider the monotonic response of the walls as the envelope of their hysteretic response ([26]). Nonetheless, a higher shear strength under cyclic loading has also been reported in the literature, for instance by Uang and Gatto [15] attributing that to the strain hardening of the staples under cyclic action.

Dolan and Madsen [27] similarly, observed a higher shear stiffness and shear strength, but for timber frame shear walls with a hardboard sheathing. It is intriguing that for OSB sheathings,

448 their observation was contradictory to the results for the case of hardboard sheathing and as a
449 consequence to the results obtained in this study. The difference between the case of OSB
450 sheathings with that of the hardboard sheathing was explained to be in the failure mode of the
451 staples being torn through the OSB panels but withdrawn in case of the hardboard sheathing.
452 As explained earlier, in this study, the governing failure mode of the staples was their
453 withdrawal from the framing members, i.e. similar to the failure mode reported in [27] for
454 hardboard sheathing.

455 *Deformation capacity and ductility ratio*

456 It is evident from the backbone curves graphed in Fig. 12 that the deformation capacity of the
457 investigated STFSWs was reduced significantly in the cyclic tests compared with the
458 monotonic ones. The amount of decrease in the deformation capacity was in the range of 19-
459 28%.

460 The ductility ratio was calculated using the equivalent elastic-plastic energy (EEEP) according
461 to ASTM E2126 [2]. As can be seen in Table 2, analogous to the deformation capacity, the
462 ductility ratio was decreased in the cyclic tests. The decrease in the ductility ratio (20-36%) was
463 higher than that in the deformation capacity. Considering the definition of the ductility ratio
464 being the ratio between the displacement capacity and the yield displacement, it can also be
465 concluded that a higher yield displacement is estimated from the cyclic tests.

466 *Viscous damping*

467 The viscous damping (v_{eq}) was calculated for each load cycle as the ratio between the
468 dissipated energy (E_d) and the maximum strain energy (E_p) according to Chopra [28] using
469 the following formula:

470 $$\nu_{eq} = \frac{1}{4\pi}\frac{E_d}{E_p}$$

The values of the equivalent viscous damping presented in Table 2 are the mean values of all cycles. The differences found between the specimens in terms of equivalent viscous damping was not significant. The values found in the present research project are in line with those published by Schädle et al. [29], who determined hysteretic equivalent viscous damping values of 10.9% – 12.9% for the first cycle and 7.9% - 9.2% for the second and third cycle.

4.3 Effect of the lateral loading protocol (ISO 21581 vs. LMS)

The low-to-moderate seismicity (LMS) loading protocol [16] was especially developed for this research project. It was therefore of interest to study the influence of this loading protocol on the seismic behavior of the investigated STFSWs and to compare the loading protocol with the ISO 21581 protocol.

As shown in Fig. 13 and reported in Table 2, the shear stiffness and the ductility, as well as the viscous damping of the walls under ISO 21581 and LMS loading protocols were fairly comparable. The main difference could be identified in the negative or unloading direction, in which a lower stiffness and strength was observed in the walls when tested under the LMS loading protocol. This difference was more highlighted in the last phases of the cyclic loading, where the difference between the applied displacements of two subsequent phases was more significant.

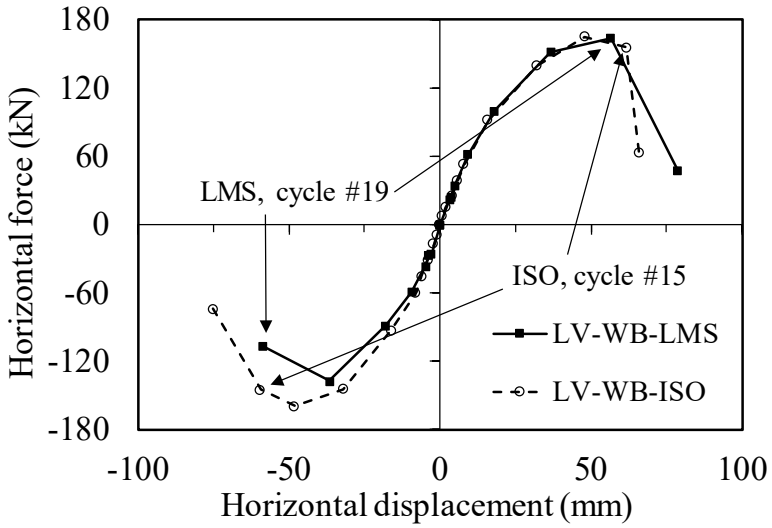

Fig. 13: Backbone envelope curves of the cyclic tests under LMS and ISO 21581 loading protocols.

In order to explain the aforementioned difference between the behavior of the walls under LMS and ISO loading protocols, since the shear strength of the STFSWs in this study was governed by the failure of staples, the difference was hypothesized to stem from various deformation demands on the staples. The 3D displacement measurement was used to examine this hypothesis. Fig. 14 illustrates the cumulative deformation of two example staples, connecting sheathing panels to the top rail (red and blue), for the studied loading protocols ISO 21581 and LMS. It must be noted that the reported displacements are not the exact deformations of the staples because the considered end points do not exactly correspond to the end points of the staples, but nevertheless they can be used as a deformation index for comparison purposes. As seen in Fig. 14b, for the test carried out under the LMS lateral loading protocol, the deformation of the left staple was extremely higher than that of the right staple at cycle 19 (the cycle in which the maximum shear resistance of the wall was reached). At this stage, withdrawal of the staples occurred on top of the left panel. By changing the loading direction, the contribution of theses staples in the lateral load carrying capacity of the wall was considerably lower resulting in an asymmetric hysteretic behavior. This phenomenon was insignificant for the test under ISO loading protocol at cycle 15 corresponding to the maximum shear resistance.

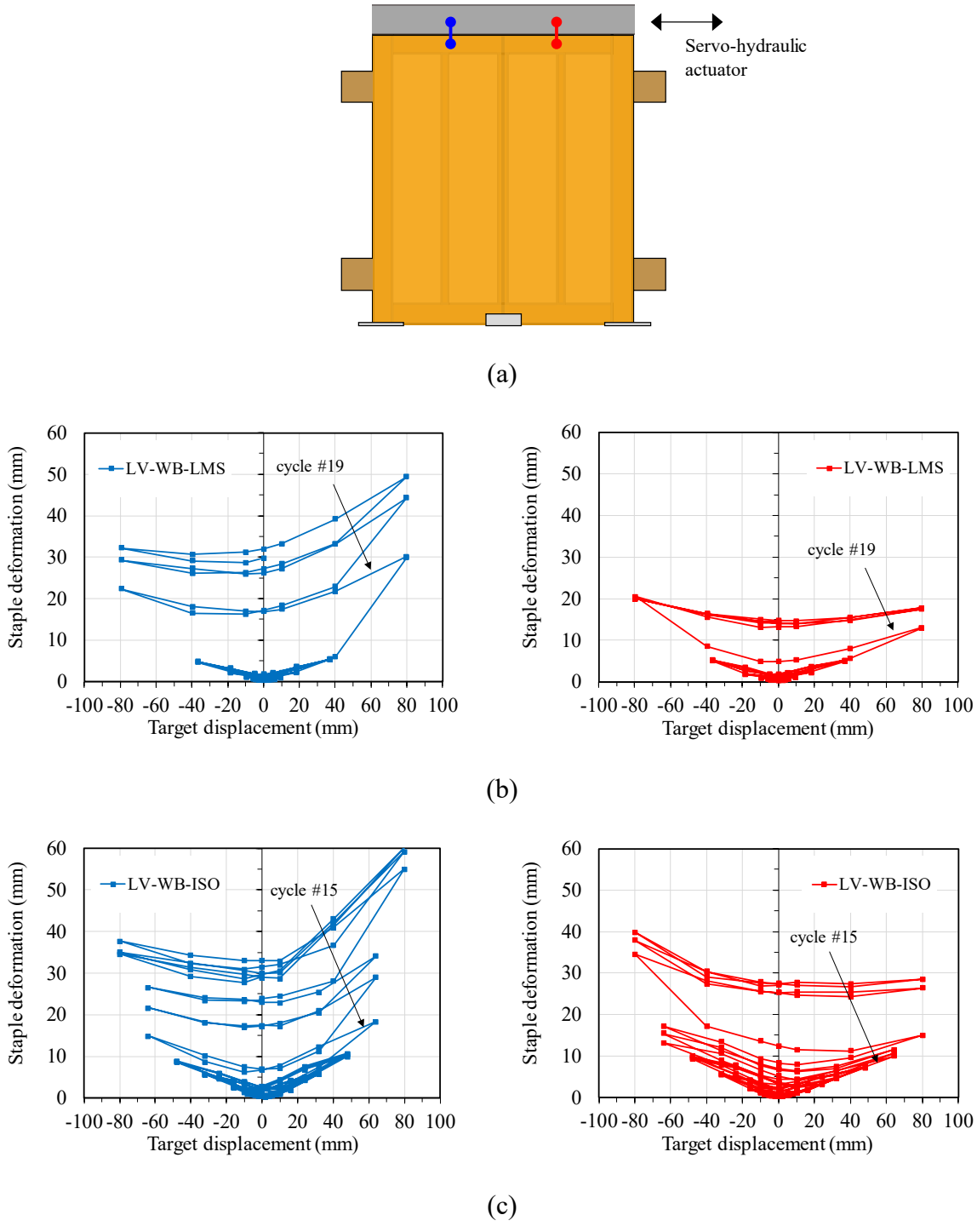

507 Fig. 14: Displacement progress of two example staples (blue and red) connecting the sheathing panel to the top
508 rail (a) subjected to the cyclic horizontal loading protocols LMS (b) and ISO 21581 (c).

509

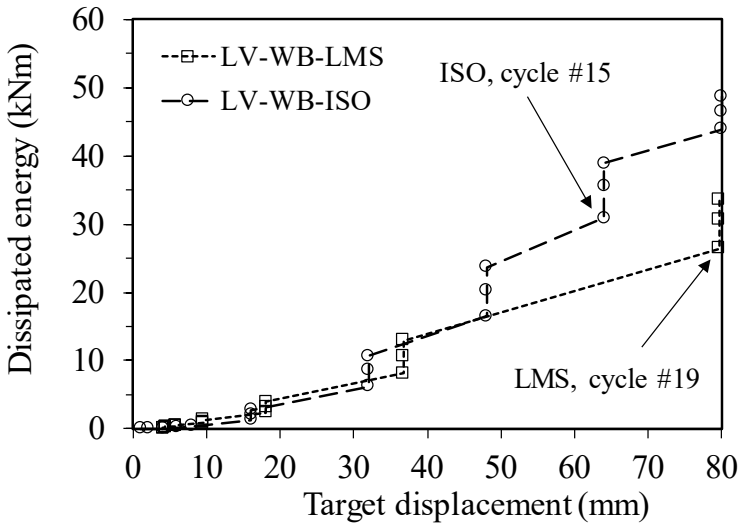

510

511 Fig. 15: Comparison of the LMS and ISO 21581 loading protocol in terms of hysteretic energy dissipation.

512

513 Another difference between the responses of the STFSWs tested under various cyclic lateral
514 loading protocols was the amount of dissipated energy. Fig. 15 illustrates the amount of energy
515 dissipation in the STFSWs tested under ISO 21581 and LMS loading protocols as a function of
516 the target displacement. At lower target displacements, both walls behaved similarly in terms
517 of energy dissipation. Under LMS loading protocol, a huge amount of energy was dissipated in
518 the cycle where the maximum shear resistance was reached and followed by withdrawal failure
519 of a large number of staples. The total amount of energy dissipated by the walls under LMS
520 loading protocol was about 30% lower than that under ISO 21581 loading protocol.

521 # 5 Conclusions

522 Sheathed timber frame shear walls (STFSW) with strong anchorage, especially designed to be
523 used as part of the (timber only) lateral force resisting system located in the perimeter of multi-
524 story timber buildings, have been described and their seismic behavior have been investigated
525 using quasi-static cyclic and monotonic tests applying different loading protocols for the
526 horizontal force. The monotonic behavior of the STFSWs has been studied and described in

detail in [1]. In this paper, their cyclic behavior has been analyzed and compared with their monotonic response. The following conclusions can be drawn:

- An up to 15% higher shear strength was observed in the sheathed timber frame shear walls under cyclic lateral loading than in the monotonic tests. Meanwhile, the deformation capacity of the walls under cyclic tests was up to 28% less than that under monotonic tests. Under monotonic lateral loading, SFTSWs with strong anchorage showed a gradual degradation of shear strength, while their behavior under cyclic loading was prominently less ductile.
- A major difference between the monotonic and cyclic responses of the walls was the lower ultimate displacement reached in the cyclic tests. The post-peak softening behavior of the walls was gradual in the monotonic tests, whereas in the cyclic ones a significant drop in the shear resistance was observed when a wall experienced a certain displacement for the second time and the third time. The inevitable result of the damage accumulation was the lower shear resistance of the walls for a certain target displacement in the post-peak range. By implementing fasteners with higher resistance against tearing out (e.g. nails with profiled shanks instead of staples) and with a more ductile steel, these problems could be overcome. Despite the resulting higher costs in the sheathing to framing connections this could be an option worthwhile checking especially when aiming at few but strong shear walls as the lateral force resisting system.
- The type of the loading protocol applied did not show a significant influence on the shear resistance and displacement capacity of the walls. The amount of energy dissipated by the wall under the LMS loading protocol was about 30% lower than that under the ISO 21581 loading protocol.

6 Acknowledgement

This study was supported by the Swiss National Science Foundation SNSF (National Research Program 66 Resource Wood, Project 406640-136900). The scientific support of Prof. Dr. Katrin Beyer, Dr. Thomas Wenk, Prof. Dr. Andrea Bernasconi, Lukas Wolf, Roland Brunner, and Andrea Sebastiani Croce is deeply appreciated. The help of the Empa technicians Heinrich Lippuner, Bruno Maag, Max Heusser, Robert Widmann, Dimitri Ott, Werner Studer, Giovanni Saragoni and Slavko Tudor in designing and assembling the test setup as well as in performing the experiments is gratefully acknowledged.

7 References

[1] Sadeghi Marzaleh A, Nerbano S, Sebastiani Croce A, Steiger R. OSB sheathed light-frame timber shear walls with strong anchorage subjected to vertical load, bending moment, and monotonic lateral load. Eng Struct. 2018;173:787-99.

[2] ASTM E2126 - 11. Standard test methods for cyclic (reversed) load test for shear resistance of vertical elements of the lateral force resisting systems for buildings. West Conshohocken, PA, United States: ASTM International; 2011.

[3] ISO 21581. Timber structures – Static and cyclic lateral load test methods for shear walls. Geneva, Switzerland: International Organization for Standardization (ISO); 2010.

[4] Casagrande D, Rossi S, Sartori T, Tomasi R. Proposal of an analytical procedure and a simplified numerical model for elastic response of single-storey timber shear-walls. Constr Build Mater. 2016;102:1101–12.

[5] Seim W, Hummel J, Vogt T. Earthquake design of timber structures – Remarks on force-based design procedures for different wall systems. Engineering Structures 2014;76:124–37.

[6] Dean P, Shenton H. Experimental investigation of the effect of vertical load on the capacity of wood shear walls. J Struct Eng. 2005;131:1104-13.

[7] Payeur M, Salenikovich A, Munoz W. Influence of vertical loads on lateral resistance and deflections of light frame shear walls. Meeting 44 of the Working Commission W18-Timber structures, CIB. Alghero, Italy, 2011, Paper CIB-W18/44-15-2.

[8] Germano F, Metelli G, Giuriani E. Experimental results on the role of sheathing-to-frame and base connections of a European timber framed shear wall. Constr Build Mater. 2015;80:315-28.

[9] Ceccotti A, Lauriola M, Pinna M and Sandhaas C. Sofie project – cyclic tests on cross-laminated wooden panels. In: Proceedings of the 9th World Conference on Timber Engineering, WCTE 2006, Portland, OR, USA, vol. 1, pp. 805–812.

[10] Grossi P, Sartori T, Tomasi R. Tests on timber frame walls under in-plane forces: part 1. Proceedings of the Institution of Civil Engineers - Structures and Buildings 2015;168:826–39.

[11] Grossi P, Sartori T, Tomasi R. Tests on timber frame walls under in-plane forces: part 2. Proceedings of the Institution of Civil Engineers - Structures and Buildings 2015;168:840–52.

[12] Dujic B, Aicher S, Zarnic R. Testing of wooden wall panels applying realistic boundary conditions. Proceedings of the 9th World Conference on Timber Engineering. Portland, Oregon, United States, 2006, p. 1186-93.

[13] Porter ML. Sequential phased displacement (SPD) procedure for TCCMAR testing. 3rd Meeting of the Joint Technical Coordinating Committee on Masonry Research. Tomamu, Japan, 1987.

[14] Krawinkler H, Parisi F, Ibarra L, Ayoub A, Medina R. Development of a testing protocol for woodframe structures. Stanford, California: Consortium of Universities for Research in Earthquake Engineering; 2001.

[15] Uang C, Gatto K. Effects of finish materials and dynamic loading on the cyclic response of woodframe shearwalls. J Struct Eng. 2003;129:1394-402.

[16] Mergos PE, Beyer K. Loading protocols for European regions of low to moderate seismicity. B EARTHQ ENG. 2014;12:2507-30.

[17] SIA 265:2012. Timber structures. Zurich, Switzerland: Swiss Society of Engineers and Architects; 2012.

[18] EN 1995-1-1. Eurocode 5: Design of timber structures - Part 1–1: General – Common rules and rules or buildings. Brussels, Belgium: European Committee for Standardization (CEN); 2004.

[19] EN 14080. Timber structures - Glued laminated timber and glued laminated solid timber - Requirements. Brussels, Belgium: European Committee for Standardization (CEN); 2013.

[20] EN 300. Oriented Strand Boards (OSB) - Definitions, classification and specifications. Brussels, Belgium: European Committee for Standardization (CEN); 2006.

[21] EN 13986. Wood-based panels for use in construction - Characteristics, evaluation of conformity and marking. Brussels, Belgium: European Committee for Standardization (CEN); 2004.

[22] Varoglu E, Karacabeyli E, Stiemer S, Ni C. Midply Wood Shear Wall System: Concept and Performance in Static and Cyclic Testing. J Struct Eng. 2006;132:1417-25.

[23] APA - The Engineered Wood Association. Builder Tip: Prevent Buckling with Proper Spacing (Form M300S). Tacoma, Washington, USA; 2013.

[24] Steiger R, Feltrin G, Weber F, Nerbano S, Motavalli M. Experimental modal analysis of a multi-storey light-frame timber building. B EARTHQ ENG. 2015.

[25] Dolan JD, Toothman AJ. Comparison of monotonic and cyclic performance of light-frame shear walls. Meeting 36 of the Working Commission W18-Timber structures, CIB. Colorado, United States, 2003, Paper CIB-W18/36-15-7.

[26] Folz B, Filiatrault A. Cyclic Analysis of Wood Shear Walls. J Struct Eng. 2001;127:433-41

[27] Dolan JD, Madsen B. Monotonic and cyclic nail connection tests. Can. J. Civ. Eng.. 1992;19:97-104.

[28] Chopra AK. Dynamics of structures: Theory and applications to earthquake engineering. Englewood Cliffs, New Jersey: Prentice-Hall; 2007.

[29] Schädle P, Blass HJ. Influence of different standards on the determination of earthquake properties of timber shear wall systems. Meeting 43 of the Working Commission W18-Timber structures, CIB. Nelson, New Zealand, 2010, Paper CIB-W18/43-15-2.